Considering the plug-flow behavior of the gas phase in nitrifying BAF models improves the prediction of N_2O emissions

Justine Fiat[1], Ahlem Filali[1,*], Yannick Fayolle[1], Jean Bernier[2], Vincent Rocher[2], Mathieu Spérandio[3], Sylvie Gillot[4]

[1] Irstea, UR HBAN, CS 10030, F-92761 Antony Cedex, France

[2] SIAAP, Direction Innovation Environnement, 92700 Colombes

[3] LISBP, Université de Toulouse, CNRS, INRA, INSA, Toulouse, France

[4] Irstea, UR REVERSAAL, F-69626 Villeurbanne Cedex, France

* Corresponding author (*ahlem.filali@irstea.fr*)

Supplementary information

A. *Characteristics of the studied BAF and model inputs*

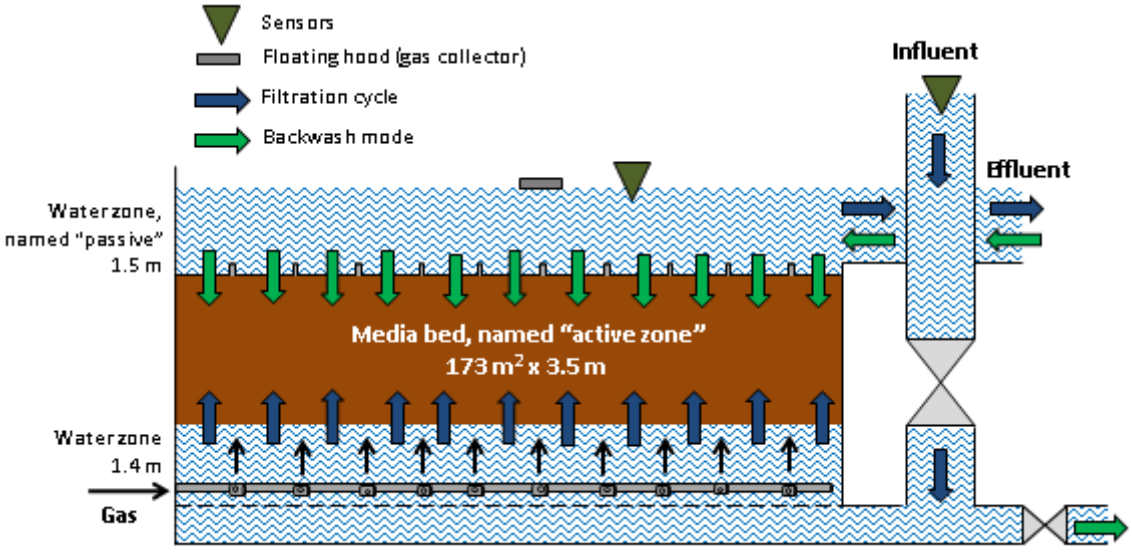

Figure S1. Schematic description of a Biostyr unit

Table S1: Main operating parameters of the BAF during the campaign (*average inputs were used for the initialization, 10-min averages were used for dynamic simulations)*.

	Q_L	Q_G	NH_4^+	NO_3^-	NO_2^-	DCO_{total}	MES	PO_4^{3-}	T	pH
	m^3/d	Nm/d	mgN/L	mgN/L	mgN/L	mg/L	mg/L	mgP/L	°C	-
Mean	20157	51333	34.8	2.5	0.19	107	35	0.51	14.5	7.5
St. dev.	4919	15309	5.1	0.5	0.04	13	8	0.17	0.9	0.4

Table S2: Effluent characteristics of the BAF during the campaign.

	NH_4^+	NO_3^-	NO_2^-	DCO	MES	PO_4^{3-}
	mgN/L	mgN/L	mgN/L	mg/L	mg/L	mgP/L
Mean	5.7	27.7	0.68	56	14	0.48
St. dev.	2.2	4.8	0.22	12	4	0.18

B. Description of the BAF model

The particle and soluble fluxes computed in the model are represented on Figure S2, and described in the following sections. The gas-liquid fluxes are not included, as they are already described in the main paper (Section 2.2.2). The compartments are not true to scale, for better clarity.

The model used in this paper was extended from a BAF model proposed by Bernier et al. (2014). It describes the functioning of a tertiary nitrifying upflow co-current Biostyr® reactor. The 3.5 meters filter bed is represented as seven reactors in series of equal height, to mimic a plug-flow reactor. This number was chosen as a compromise between correct flow representation and reasonable calculation time. Each reactor is composed of four compartments: the liquid phase that is considered biologically inactive – biomass concentrations being negligible compared to those in the biofilm, – the gas phase, the inert media, and two biofilm layers: the basal layer (close to the media), and the surface one (in contact with water). These compartments are modelled as completely stirred tank reactors (CSTR). An additional CSTR is modeled to represent the 1.5 meter overflow (see Figure S1).

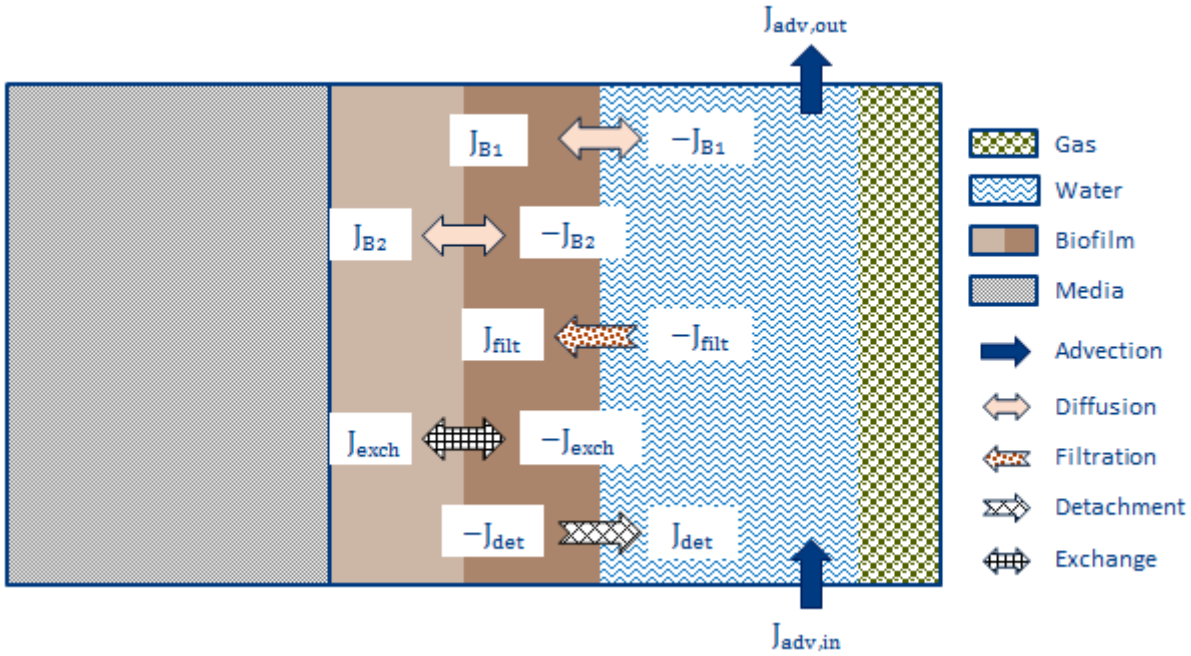

Figure S2: Schematic representation of one of the seven reactors in the series and the associated fluxes (except fluxes related to the gas phase).

B.1. Biofilm representation

The media presence and the expansion of the biofilm reduce the volume accessible to the water flow. The media fraction is constant (64% of the active zone), while the biofilm fraction is variable and can be calculated from the biofilm thickness, and the media specific area [Eq.S1]. The biofilm thickness in a given reactor n is equal to the sum of all biofilm layer thicknesses [Eq.S2] (in this work, k=2). The biofilm thickness varies with the filtration of particles (attachment), detachment and net biomass growth. It is estimated based on the density of the dry biofilm, the maximum biofilm thickness and the local TSS concentration [Eq.S3]. The factor ICV is used to convert the sum of particle concentrations from COD to TSS. In other words, a biofilm layer is considered as full when the concentration of particles reaches its maximal value (which corresponds to the density of

the dry biofilm). This maximum thickness is calculated from the constant maximum deposit fraction on the media [Eq.S4].

[Eq.S1] $$\varepsilon_{B,n} = Z_n a_a$$

[Eq.S2] $$Z_n = \sum_{j=1}^{k} Z_{j,n}$$

[Eq.S3] $$Z_{j,n} = \frac{\sum X_{j,n} / ICV}{\rho_B} Z_{max,j}$$

[Eq.S4] $$Z_{max,j} = \frac{Z_{max}}{k}$$

where ε_B is the biofilm fraction, Z and Z_j (m) respectively the total biofilm thickness in reactor, and the biofilm thickness in a given biofilm layer, Z_{max} and $Z_{max,j}$ (m) their respective maximum values, ΣX_j the sum of particle concentrations in a biofilm layer ($gCOD/m^3$), ICV the conversion factor from COD to TSS (1.5 gCOD/gTSS), ρ_B, the dry biofilm density (g/m^3) and k the number of biofilm layers. n stands for the reactor number, and j for the biofilm layer.

B.2. Fate of particles

The mass balances of a particulate compound X_i in the liquid, the surface biofilm layer (B1) and the basal biofilm layer (B2) of a reactor n are given in Eq. [S5], [S6] and [S7], respectively. Particles can be filtered, detached, or exchanged.

[Eq.S5] $$V_{L,n} \frac{\partial X_{i,L,n}}{\partial t} = J_{Xi,adv,in,n} - J_{Xi,adv,out,n} - J_{Xi,filt,n} + J_{Xi,det,n}$$

[Eq.S6] $$V_{B1,n}\frac{\partial X_{i,B1,n}}{\partial t} = J_{Xi,filt,n} - J_{Xi,det,n} - J_{Xi,exch,n} + V_{B1,n}r_{i,B1,n}$$

[Eq.S7] $$V_{B2,n}\frac{\partial X_{i,B2,n}}{\partial t} = J_{Xi,exch,n} + V_{B2,n}r_{i,B2,n}$$

70

71 Where X (g/m^3) is the concentration of a given particulate compound, V_{B1} and V_{B2}
72 (m^3) are the surface and basal biofilm layer volumes, respectively. For simplification, they
73 were considered equal to their maximum value (7.35 m^3). The terms r_{B1} and r_{B2} ($g/m^3/d$)
74 stand for the sum of reaction rates involving a given X_i. J_{adv} (g/d) is the flux entering (in)
75 or leaving (out) the reactor. J_{filt} (g/d) is the flux retained in the surface biofilm layer by
76 filtration [Eq.S8]. The filtration coefficient is calculated from an empirical relation [Eq.S9],
77 which involves the deposit fraction on the media [Eq.10], J_{det} (g/d) is the flux detached
78 from the surface layer to the bulk [Eq.S11]. J_{exch} (g/d) is the flux leaving the surface for the
79 basal layer [Eq.S12]. i and n stand for the component and the reactor respectively.

80

[Eq.S8] $$J_{Xi,filt,n} = \frac{\lambda u X_{i,L,n} V_{R,n}}{1 - \sum X_{bulk,n}/\rho_B}$$

[Eq.S9] $$\lambda = \lambda_0 \left(1 + \frac{\beta\sigma}{\varepsilon_0}\right)^y \left(1 - \frac{\sigma}{\varepsilon_0}\right)^z \left(1 - \frac{\sigma}{\sigma_{max}}\right)^x$$

[Eq.S10] $$\sigma = a_a Z_n$$

[Eq.S11] $$J_{Xi,det,n} = k_{det} a_a V_{R,n} \frac{X_{i,B1,n}}{\sum X_{B1,n}}$$

[Eq.S12] $$J_{Xi,exch,n} = k_{exc} a_a V_{R,n} (\Sigma X_{B1,n} - \Sigma X_{B2,n})$$

81

82 where λ and λ_0 are the filtration and the clean filtration coefficients, u ($m^3/m^2/d$) the
83 surface liquid flowrate, x, y and z empirical constants calibrated in a previous work
84 (Bernier et al. 2014), σ the biofilm deposit fraction, a_a is the media specific area (1000

m^2/m^3 of empty reactor), k_{det} ($g/m^2/d$) the detachment coefficient, and k_{exc} (m/d) the exchange coefficient.

B.3. Fate of soluble components

The mass balances of a soluble component S_i in the liquid, the surface biofilm layer and the basal biofilm layer of a reactor n are given in Eq. [S13], [S14] and [S15], respectively. A soluble can enter or leave a reactor by advection, and diffuse between compartments.

[Eq.S13] $$V_{L,n}\frac{\partial S_{i,L,n}}{\partial t} = J_{Si,adv,in,n} - J_{Si,adv,out,n} - J_{Si,B1,n}$$

[Eq.S14] $$V_{B1,n}\frac{\partial S_{i,B1,n}}{\partial t} = J_{Si,B1,n} - J_{Si,B2,n} + V_{B1,n}r_{i,B1,n}$$

[Eq.S15] $$V_{B2,n}\frac{\partial S_{i,B2,n}}{\partial t} = J_{Si,B2,n} + V_{B1}r_{i,B2,n}$$

where S (g/m^3) is the concentration of a given soluble compound, J_{B1} (g/d) the flux diffused from the liquid to the surface layer [Eq.S16], and J_{B2} (g/d) the flux diffused from the surface to the basal biofilm layer [Eq.S17]. The resistance to transfer is modeled by a constant thickness liquid film. A reduction factor is included to better describe the diffusion into the biofilm compared to water.

[Eq.S16] $$J_{Si,B1,n} = \frac{D_i f_D}{L_f} a_a V_{R,n}\left(S_{i,bulk,n} - S_{B1,n}\right)$$

[Eq.S17] $$J_{Si,B2,n} = \frac{D_i f_D}{Z_{1,n}} a_a V_{R,n}\left(S_{B1,n} - S_{B2,n}\right)$$

where D (m^2/d) is the diffusion coefficient in water, f_D the reduction factor of diffusion in the biofilm compared to water, L_f (m) the thickness of the liquid film. It was calculated for each soluble from its Sherwood number [Eq.S18], and the average 100 µm value was chosen.

[Eq.S18] $$L_f = \frac{d_{eq}}{Sh}$$

[Eq.S19] $$Sh = 2 + 0.51 * \left(4.23 Re^{5/6}\right)^{0.6} Sc^{1/3}$$

[Eq.S20] $$Re = \frac{u d_{eq}}{\nu \varepsilon_0}$$

[Eq.S21] $$Sc = \frac{\nu}{D_i}$$

where ν (m^2/s) is the kinetic viscosity of water, d_{eq} (m) the average diameter of the media beads, Sh, Sc and Re the Sherwood, Schmidt and Reynolds numbers (adimensional). Their values, calculated on the 14-day studied period, are reported in Table S1 for each soluble component.

Table S1: Average liquid film thickness calculated for each soluble component

S_i	D_i (m^2/d)	Sc (-)	Sh (-)	**L_f (µm)**
S_{alk}	1.73E-04	654	38	**106**
S_S	8.64E-05	1307	47	**85**
S_i	8.64E-05	1307	47	**85**
S_{no3}	1.73E-04	654	38	**106**
S_{n2}	1.64E-04	688	38	**104**
S_{nd}	8.64E-05	1307	47	**85**
S_{nh}	2.16E-04	523	35	**114**
S_{po}	2.16E-04	523	35	**114**
S_{no2}	1.81E-04	623	37	**107**
S_o	2.16E-04	523	35	**114**
S_{nh2oh}	1.87E-04	605	37	**108**
S_{no}	1.91E-04	591	37	**109**
S_{n2o}	2.22E-04	509	35	**115**

B.4. Backwash events

Backwash activation and deactivation is an input of the model (0 and 1 signal), and impacts each reactor in series independently. To maintain enough biomass for pollution elimination, lower extraction efficiency is implemented for biomass than for non-biomass particles (1% against 20%). For simplification, the model does not consider a homogenization of biomass concentrations in the biofilter during a backwash cycle.

C. Description of the biokinetic model

C.1. Biological pathways

The nitrification model was originally modified from the ASM1 (Bernier et al. 2014) to divide it into the oxidation of NH_4^+ to NO_2^- (nitritation) by AOBs, and the oxidation of NO_2^- to NO_3^- (nitratation) by NOBs. In this work, nitrification was extended to include nitrification intermediates NH_2OH and NO, and the production of N_2O according to Pocquet et al. (2016) *via* the NN and ND pathways (Figure S3).

Most kinetic parameters were taken from the original model (Bernier et al. 2014). For the added reactions, parameters were taken from the second case of study of Lang et al. (2016). Authors calibrated the model from Pocquet et al. (2016) on a dataset much closer to experimental conditions found on Seine Aval (low nitrite concentrations).

The nitrification stage of the Seine Aval WRRF is preceded by a carbon elimination stage. Consequently, aerobic and anoxic heterotrophic growths were considered in the model. Originally, denitrification was described as a 2-step reaction ($NO_3^- \rightarrow NO_2^- \rightarrow N_2$) In this work, we considered a 4 step-denitrification reaction according to Hiatt and Grady (2008) ($NO_3^- \rightarrow NO_2^- \rightarrow NO \rightarrow N_2$) to account for a possible contribution of heterotrophs to the production and/or consumption of N_2O (Figure S3). The average influent soluble COD being 21.7 gCOD/m^3, heterotrophs can growth (Y_h = 0.67 gCOD/gCOD).

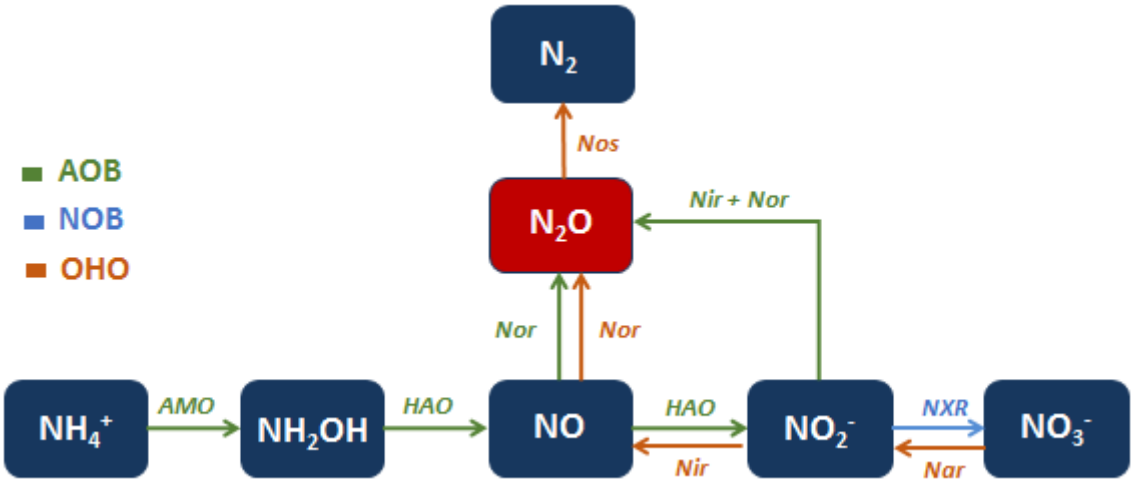

Figure S3: Schematic representation of biological pathways included in the extended BAF model. Acronyms AMO, HAO, NXR, Nar, Nir, Nor and Nos stand for the enzymes ammonium monooxygenase, hydroxylamine oxidoreductase, nitrite oxidoreductase, nitrate reductase, nitrite reductase, and NO reductase and N_2 synthase.

C.2. Gujer matrix

Table S2: Gujer matrix of the heterotrophic denitrification model

Process	S_S	X_S	X_{BH}	X_P	S_O	S_{NH4}	S_{NO}	S_{NO2}	S_{N2O}	S_{NO3}	S_{N2}	S_{PO}	S_{ALK}
R1	$-\frac{1}{Y_h}$		1		$-\frac{(1-Y_h)}{Y_h}$	$-ixbn$						$-ixbp$	$-\frac{ixbn}{14}$
R2	$-\frac{1}{\eta_Y Y_h}$		1			$-ixbn$		B		$-B$		$-ixbp$	$-\frac{ixbn}{14}$
R3	$-\frac{1}{\eta_Y Y_h}$		1			$-ixbn$	A	$-A$				$-ixbp$	$\frac{(1-\eta yYh)}{(14*4/7*\eta yYh)}-\frac{ixbn}{14}$
R4	$-\frac{1}{\eta_Y Y_h}$		1			$-ixbn$	$-A$		A			$-ixbp$	$-\frac{ixbn}{14}$
R5	$-\frac{1}{\eta_Y Y_h}$		1			$-ixbn$			$-A$		A	$-ixbp$	$-\frac{ixbn}{14}$
R6		$1-f_p$	-1	f_p								$-ixbp$	

$$A=\frac{(1-\eta yYh)}{(4/7*\eta yYh)}\ ;B=\frac{(1-\eta yYh)}{(8/7*\eta yYh)}$$

148 **Table S3: Kinetic rates of the heterotrophic denitrification model**

Process	Kinetic rate
R1 = Aerobic growth heterotrophs	$\mu_{H,max}\left(\frac{S_S}{S_S+K_S}\right)\left(\frac{S_O}{S_O+K_{O,H}}\right)\left(\frac{S_{PO}}{S_{PO}+K_{PO}}\right)X_{BH}$
R2 = Anoxic growth heterotrophs (NO_3^-)	$\eta_{H1}\mu_{H,max}\left(\frac{S_S}{S_S+K_{S,1}}\right)\left(\frac{K_{I,O,H,1}}{S_O+K_{I,O,H,1}}\right)\left(\frac{S_{NO3}}{S_{NO3}+K_{H,NO3}}\right)\left(\frac{S_{PO}}{S_{PO}+K_{PO}}\right)X_{BH}$
R3 = Anoxic growth of heterotrophs (NO_2^-)	$\eta_{H2}\mu_{H,max}\left(\frac{S_S}{S_S+K_{S,2}}\right)\left(\frac{K_{I,O,H,2}}{S_O+K_{I,O,H,2}}\right)\left(\frac{S_{NO2}}{S_{NO2}+K_{H,NO2}}\right)\left(\frac{K_{I,NO,2}}{S_{NO}+K_{I,NO,2}}\right)\left(\frac{S_{PO}}{S_{PO}+K_{PO}}\right)X_{BH}$
R4 = Anoxic growth of heterotrophs (NO)	$\eta_{H3}\mu_{H,max}\left(\frac{S_S}{S_S+K_{S,3}}\right)\left(\frac{K_{I,O,H,3}}{S_O+K_{I,O,H,3}}\right)\left(\frac{S_{NO}}{S_{NO}+K_{H,NO}+S_{NO}^2/K_{I,NO,3}}\right)\left(\frac{S_{PO}}{S_{PO}+K_{PO}}\right)X_{BH}$
R5 = Anoxic growth of heterotrophs (N_2O)	$\eta_{H4}\mu_{H,max}\left(\frac{S_S}{S_S+K_{S,4}}\right)\left(\frac{K_{I,O,H,4}}{S_O+K_{I,O,H,4}}\right)\left(\frac{S_{N2O}}{S_{N2O}+K_{H,N2O}}\right)\left(\frac{K_{I,NO,4}}{S_{NO}+K_{I,NO,4}}\right)\left(\frac{S_{PO}}{S_{PO}+K_{PO}}\right)X_{BH}$
R6 = Decay of heterotrophs	$b_H X_{BH}$

149

150

Table S4: Gujer matrix of the nitrification model

Process	S_S	X_S	X_{AOB}	X_{NOB}	X_P	S_O	S_{NH4}	S_{NH2OH}	S_{NO}	S_{NO2}	S_{N2O}	S_{NO3}	S_{ND}	X_{ND}	S_{PO}	S_{ALK}
R7						$-8/7$	-1	1								$-\frac{1}{14}$
R8			1			$-\frac{(12/7-\text{Yaob})}{\text{Yaob}}$	$-\text{ixbn}$	$-\frac{1}{\text{Yaob}}$	$\frac{1}{\text{Yaob}}$						$-\text{ixbp}$	$-\frac{\text{ixbn}}{14}$
R9						$-4/7$			-1	1						$-\frac{1}{14}$
R10								-1	-4	1	4					$-\frac{1}{14}$
R11								-1		-1	2					$\frac{1}{14}$
R12				1		$-\frac{(16/14-\text{Ynob})}{\text{Ynob}}$	$-\text{ixbn}$			$-\frac{1}{\text{Ynob}}$		$\frac{1}{\text{Ynob}}$			$-\text{ixbp}$	$-\frac{\text{ixbn}}{14}$
R13		$1-f_p$	-1		f_p									$\text{ixbn}-\text{fp}*\text{ixun}$	$\text{ixbp}-\text{fp}*\text{ixup}$	
R14		$1-f_p$		-1	f_p									$\text{ixbn}-\text{fp}*\text{ixun}$	$\text{ixbp}-\text{fp}*\text{ixup}$	
R15							1						-1			$\frac{1}{14}$
R16	1	-1														
R17													1	-1		

Table S5: Kinetic rates of the nitrification model

Process	Kinetic rate
R7 = Oxidation of NH_4 to NH_2OH	$\left(\frac{\mu_{AOB}}{Y_{AOB}}\right)\left(\frac{S_O}{S_O + K_{O,AOB,1}}\right)\left(\frac{S_{NH4}}{S_{NH4} + K_{NH4,AOB}}\right)X_{AOB}$
R8 = Growth of AOB	$\mu_{AOB}\left(\frac{S_O}{S_O + K_{O,AOB,2}}\right)\left(\frac{S_{NH4}}{S_{NH4} + 10^{-12}}\right)\left(\frac{S_{NH2OH}}{S_{NH2OH} + K_{NH2OH}}\right)\left(\frac{S_{PO}}{S_{PO} + K_{PO}}\right)X_{AOB}$
R9 = Oxidation of NO to NO_2^-	$\left(\frac{\mu_{AOB}}{Y_{AOB}}\right)\left(\frac{S_O}{S_O + K_{O,AOB,2}}\right)\left(\frac{S_{NO}}{S_{NO} + K_{NO,AOB,HAO}}\right)X_{AOB}$
R10 = Reduction of NO to N_2O	$\eta_{NN}\left(\frac{\mu_{AOB}}{Y_{AOB}}\right)\left(\frac{S_{NH2OH}}{S_{NH2OH} + K_{NH2OH}}\right)\left(\frac{S_{NO}}{S_{NO} + K_{NO,AOB,NN}}\right)X_{AOB}$
R11 = Reduction of NO_2 to N_2O	$\eta_{ND}\left(\frac{\mu_{AOB}}{Y_{AOB}}\right)\left(\frac{S_{NH2OH}}{S_{NH2OH} + K_{NH2OH}}\right)\left(\frac{S_{NO2}}{S_{NO2} + K_{NO2,AOB}}\right)DO_{Haldane}X_{AOB}$
R12 = Growth of NOB	$\mu_{NOB,max}\left(\frac{S_O}{S_O + K_{O,NOB}}\right)\left(\frac{S_{NO2}}{S_{NO2} + K_{NO2,NOB}}\right)\left(\frac{S_{PO}}{S_{PO} + K_{PO}}\right)X_{NOB}$
R13 = Decay of AOB	$b_{AOB}X_{AOB}$
R14 = Decay of NOB	$b_{NOB}X_{NOB}$
R15 = Ammonification	$k_a S_{ND} X_{BH}$
R16 = Hydrolysis	$k_H\left(\frac{X_S/X_{BH}}{K_X + X_S/X_{BH}}\right)\left[\left(\frac{S_O}{S_O + K_{O,H}}\right) + \eta_h\left(\frac{K_{O,H}}{S_O + K_{O,H}}\right)\left(\frac{\sum S_{NOX}}{H_{H,NO3} + \sum S_{NOX}}\right)\right]X_{BH}$
R17 = N hydrolysis	$k_H\left(\frac{X_{ND}}{X_S}\right)\left(\frac{X_S/X_{BH}}{K_X + X_S/X_{BH}}\right)\left[\left(\frac{S_O}{S_O + K_{O,H}}\right) + \eta_h\left(\frac{K_{O,H}}{S_O + K_{O,H}}\right)\left(\frac{\sum S_{NOX}}{H_{H,NO3} + \sum S_{NOX}}\right)\right]X_{BH}$

D. List of parameters used in the BAF model

Table S6: List of parameters defined in the extended BAF model. [a] Bernier et al. (2014), [b] Hiatt and Grady (2008), [c] Lang et al. (2016), [d] Sander (2015), [e] Pocquet et al. (2016), [f] Vigne et al. (2010), [g] Sabba et al. (2017), * corrected from original publication.

Fractionation parameters			
Parameter	**Description**	**Value**	**Source**
DCOX/MVS	Particular COD to VSS ratio	1.5 gCOD/gVSS	[a]
MVS/MES	VSS to TSS ratio	0.75 gTSS/gVSS	[a]
TKN/NH4	TKN to NH4 ratio	1.1 gN/gN	[a]
frssi	Inert fraction of soluble COD	0.65 gCOD/gCOD	[a]
frxxi	Inert fraction of particular COD	0.65 gCOD/gCOD	[a]
frxu	Inactive biomass fraction of particular COD	0 gCOD/gCOD	[a]
frbh	Heterotrophic biomass fraction of particular COD	0.25 gCOD/gCOD	[a]
frbai	AOB fraction of particular COD	0 gCOD/gCOD	[a]
frbaa	NOB fraction of particular COD	0 gCOD/gCOD	[a]
frxnd	Particular fraction of organic N	0.45 gCOD/gCOD	[a]
ASM parameters			
b_{AOB}	Decay coefficient, AOB	0.17 d^{-1}	[a]
b_{NOB}	Decay coefficient, NOB	0.17 d^{-1}	[a]
b_H	Decay coefficient, heterotrophs	0.62 d^{-1}	[a]
η_H	Anoxic hydrolysis factor	0.4	[a]
η_{H1}	Anoxic growth factor for heterotrophs, NO_3^-	0.28	[b]
η_{H2}	Anoxic growth factor for heterotrophs, NO_2^-	0.16	[b]
η_{H3}	Anoxic growth factor for heterotrophs, NO	0.35	[b]
η_{H4}	Anoxic growth factor for heterotrophs, N_2O	0.35	[b]
η_{ND}	Reduction factor for the ND pathway	0.1056	[c]
η_{NN}	Reduction factor for the NN pathway	0.07693	[c]
η_Y	Anoxic yield factor	0.75	[a]
ixbn	Mass of nitrogen per mass of COD in active biomass	0.086 gN/gCOD	[a] [b]
ixun	Mass of nitrogen per mass of COD in biomass debris	0.06 gN/gCOD	[a] [b]
ixbp	Mass of phosphorus per mass of COD in active biomass	0.015 gP/gCOD	[a]
ixup	Mass of phosphorus per mass of COD in biomass debris	0.015 gP/gCOD	[a]
f_p	Fraction of active biomass contributing to biomass debris	0.08 gN/gCOD	[a] [b]
k_a	Ammonification rate coefficient	0.08 m^3/(gCOD.d)	[a]
k_h	Hydrolysis coefficient	3 gCOD/(gCOD.d)	[a]
$K_{H,NO3}$	Half-saturation coefficient for NO_3^-, heterotrophs (gN/m^3)	0.2 gN/m^3	[a] [b]
$K_{H,NO2}$	Half-saturation coefficient for NO_2^-, heterotrophs (gN/m^3)	0.2 gN/m^3	[a] [b]

$K_{H,NO}$	Half-saturation coefficient for NO, heterotrophs	0.05 gN/m^3	[b]
$K_{H,N2O}$	Half-saturation coefficient for N_2O, heterotrophs	0.05 gN/m^3	[b]
$K_{HNO2,AOB}$	AOB affinity constant for HNO_2	0.00073 gN/m^3	[c]
$K_{I,NO,2}$	NO inhibition coefficient, NO_2^-	0.5 gN/m^3	[a] [b]
$K_{I,NO,3}$	NO inhibition coefficient, NO	0.3 gN/m^3	[a] [b]
$K_{I,NO,4}$	NO inhibition coefficient, N_2O	0.075 gN/m^3	[a] [b]
$K_{I,O,AOB}$	Inhibition constant by O_2 on N_2O production	4.5 gO_2/m^3	[c]
K_{NH2OH}	AOB affinity constant for NH_2OH	0.0147 gN/m^3	Calculated
$K_{NH4,AOB}$	AOB affinity constant for NH_4	1 gN/m^3	[a]
$K_{NO,AOB,HAO}$	AOB affinity constant for NO from HAO	0.0003 gN/m^3	[c]
$K_{NO,AOB,NN}$	AOB affinity constant for NO from NirK	0.008 gN/m^3	[c]
$K_{NO2,NOB}$	Half-saturation coefficient for NO_2^-, NOB	0.2 gN/m^3	[a]
$K_{O,AOB,1}$	AOB affinity constant for O_2 (AMO reaction)	0.48 gO_2/m^3	[a]
$K_{O,AOB,2}$	AOB affinity constant for O_2 (HAO reactions)	0.3 gO_2/m^3	[c]
$K_{O,AOB,ND}$	AOB constant for O_2 effect on the ND pathway	0.019 gO_2/m^3	[c]
K_{OH}	Half-saturation coefficient for O_2, heterotrophs	0.1 gO_2/m^3	[a] [b]
$K_{I,OH,1}$	Inhibition coefficient for O_2, heterotrophs, NO_3^-	0.1 gO_2/m^3	[a] [b]
$K_{I,OH,2}$	Inhibition coefficient for O_2, heterotrophs, NO_2^-	0.1 gO_2/m^3	[b]
$K_{I,OH,3}$	Inhibition coefficient for O_2, heterotrophs, NO	0.1 gO_2/m^3	[b]
$K_{I,OH,4}$	Inhibition coefficient for O_2, heterotrophs, N_2O	0.1 gO_2/m^3	[b]
$K_{O,NOB}$	NOB affinity constant for O_2	0.6 gO_2/m^3	[a]
K_{PO}	Half-saturation coefficient for orthophosphate	0.01 gP/m^3	[a]
K_S	Half-saturation coefficient for substrate, heterotrophs	20 $gCOD/m^3$	[b]
K_{S1}	Half-saturation coefficient for substrate, heterotrophs, NO_3^-	20 $gCOD/m^3$	[b]
K_{S2}	Half-saturation coefficient for substrate, heterotrophs, NO_2^-	20 $gCOD/m^3$	[b]
K_{S3}	Half-saturation coefficient for substrate, heterotrophs, NO	20 $gCOD/m^3$	[b]
K_{S4}	Half-saturation coefficient for substrate, heterotrophs, N_2O	40 $gCOD/m^3$	[b]
K_x	Half-saturation coefficient for hydrolysis of slowly biodegradable substrate	0.03 gCOD/g biomass COD	[a]
μ_{AOB}	Maximum specific growth rate for AOB	0.8 d^{-1}	[a]
μ_{NOB}	Maximum specific growth rate for NOB	1 d^{-1}	[a]
μ_H	Maximum specific growth rate for heterotrophs	6 d^{-1}	[a]
Y_{AOB}	Autotrophic yield, AOB	0.21 gCOD/gN	[a]
Y_{NOB}	Autotrophic yield, NOB	0.06 gCOD/gN	[a] [b]
Y_H	Heterotrophic yield	0.666 gCOD/gN	[a]
Physical parameters			
a_a	Media specific are	1000 m^2/m^3 of empty filter	[a]
ε_0	Media initial porosity	0.356	[a]
S	Media bed area	173 m^2	[a]
H_{media}	Media bed height	3.5 m	[a]

$H_{surverse}$	Water height above media	1.5 m	[a]
$H_{sousverse}$	Water height under media	1.6 m	[a]
D_p	Media particles mean diameter	0.004 m	[a]
NBR	Number of reactors	7	[a]
NBL	Number of biofilm layers	2	[a]
icv	COD to TSS ratio in biofilm	1.5 gCOD/gTSS	[a]
k_{det}	Biofilm detachment level	1 g/(m².d)	[a]
ρ_B	Biofilm dry density	100200 g/m^3	[a]
σ_u	Max specific deposit around media	0.17	[a]
Backwash parameters			
$k_{back,B}$	Extraction efficiency for biomass, backwash	0.01 d^{-1}	[a]
$k_{back,NB}$	Extraction efficiency for non-biomass, backwash	0.2 d^{-1}	[a]
Filtration parameters			
β	Media packing factor	1.95	[a]
λ_0	Clean filter filtration coefficient	0.0006	[a]
x	x filter constant	1	[a]
y	y filter constant	3	[a]
z	z filter constant	0.375	[a]
Transfer parameters			
F	Fouling factor for aeration	1	[a]
α	Efficiency factor for aeration in wastewater	0.95	[a]
β_0	Factor for oxygen solubility	0.95	[a]
KH_{O2}	Henry's law constant for O_2 at 20°C	41.6 gO_2/(m^3.atm)	[d]
KH_{NO}	Henry's law constant for NO at 20°C	26.6 gN-NO/(m^3.atm)	[d]
KH_{N2O}	Henry's law constant for N_2O at 20°C	700 gN-N_2O/(m^3.atm)	[d]
KH_{N2}	Henry's law constant for N_2 at 20°C	16.8 gN-N_2/(m^3.atm)	[d]
ρ_O	Partial pressure of O_2	0.21 atm	Calculated
ρ_{NO}	Partial pressure of NO	0 atm	Calculated
ρ_{N2O}	Partial pressure of N_2O	3.28E-07 atm	Calculated
ρ_{N2}	Partial pressure of N_2	0.78 atm	Calculated
Diffusion parameters			
DS_{alk}	Alkalinity diffusion coefficient	1.73E-04 m²/d	[f]
DS_s	Soluble substrate diffusion coefficient	8.64E-05 m²/d	[f]
DS_i	Inert diffusion coefficient	8.64E-05 m²/d	[f]
DS_{no3}	NO_3^- diffusion coefficient	1.73E-04 m²/d	[f]
DS_{n2}	N_2 diffusion coefficient	1.64E-04 m²/d	[f]
DS_{nd}	Soluble nitrogen diffusion coefficient	8.64E-05 m²/d	[f]
DS_{nh}	Ammonia diffusion coefficient	2.16E-04 m²/d	[f]
DS_{po}	Orthophosphates diffusion coefficient	2.16E-04 m²/d	[a]*

DS_{no2}	NO_2^- diffusion coefficient	1.81E-04 m^2/d	[a]*
DS_o	Dissolved oxygen diffusion coefficient	2.16E-04 m^2/d	[f]
DS_{nh2oh}	Hydroxylamine diffusion coefficient	1.87E-04 m^2/d	[g]
DS_{no}	NO diffusion coefficient	1.91E-04 m^2/d	[g]
DS_{n2o}	Nitrous oxide diffusion coefficient	2.22E-04 m^2/d	[g]
f_D	Diffusion reduction factor in biofilm	0.7	[a]
L_f	Liquid film thickness	100 µm	Calculated
k_{exc}	Particular matter exchange coefficient	0.00002 m/d	[a]
Temperature parameters			
$\theta_{\mu H}$	Temperature effect on heterotroph growth	1.072	[a]
θ_{bH}	Temperature effect on heterotroph decay	1.029	[a]
$\theta_{\mu AOB}$	Temperature effect on AOB growth	1.078	[a]
θ_{bAOB}	Temperature effect on AOB decay	1.029	[a]
$\theta_{\mu NOB}$	Temperature effect on NOB growth	1,09	[a]
θ_{bNOB}	Temperature effect on NOB decay	1.029	[a]
θ_{ka}	Temperature effect on ammonification	1.072	[a]
θ_{kH}	Temperature effect on hydrolysis	1.072	[a]
θ_{kLa}	Temperature effect on k_La	1.005	[a]

E. Simulation results from the "base" model

The dynamic predictions of effluent NH_4^+ and NO_3^- concentrations are presented on Figure S4. Nitrification is correctly predicted (both order of magnitude and dynamics).

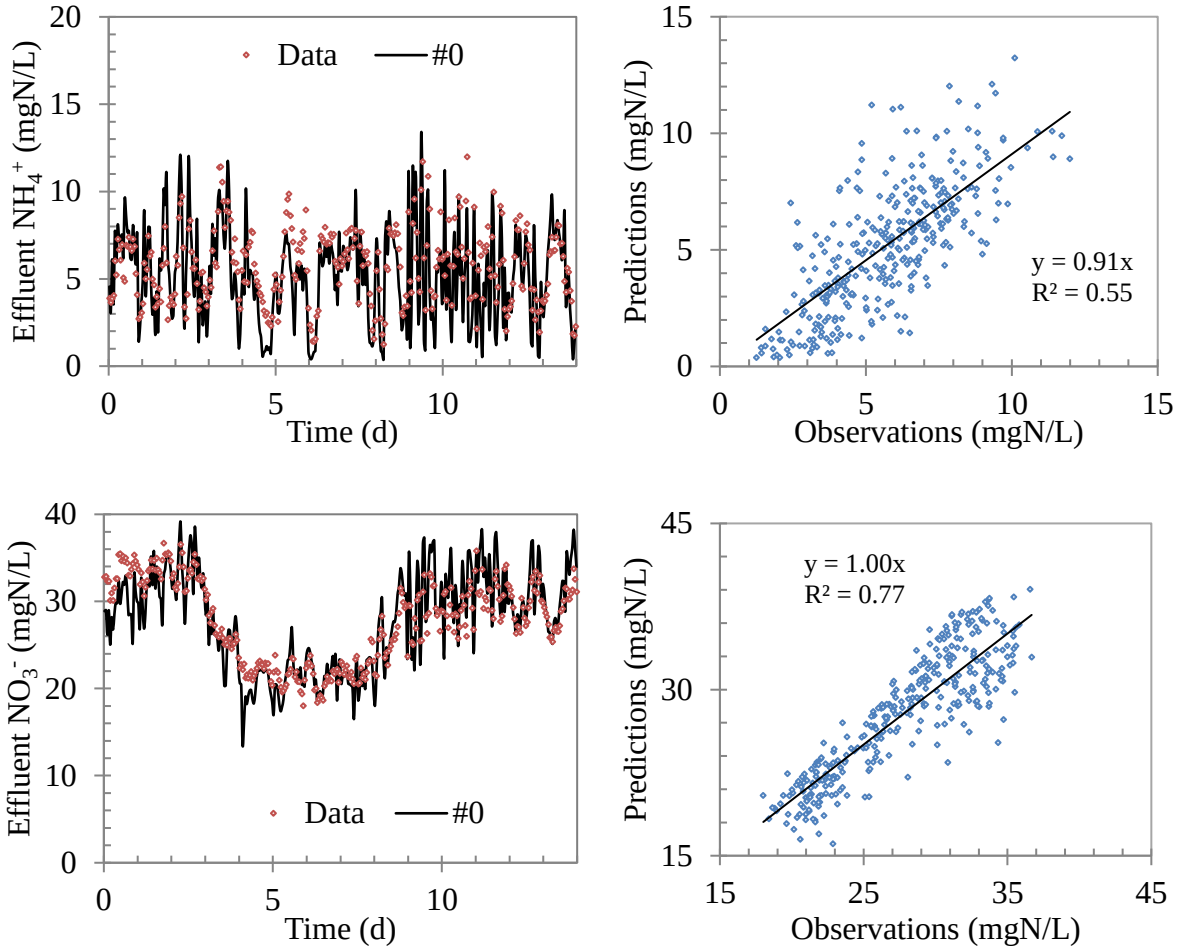

Figure S4: effluent NH_4^+ (top panel) and NO_3^- (bottom panel) predictions and experimental data.

References

Bernier, J., V. Rocher, S. Guerin, and P. Lessard. 2014. Modelling the nitrification in a full-scale tertiary biological aerated filter unit. *Bioprocess and Biosystems Engineering* 37 (2):289-300.

Gillot, S., F. Kies, C. Amiel, M. Roustan, and A. Heduit. 2005. Application of the off-gas method to the measurement of oxygen transfer in biofilters. *Chemical Engineering Science* 60 (22):6336-6345.

Hiatt, W. C., and C. P. L. Grady. 2008. An Updated Process Model for Carbon Oxidation, Nitrification, and Denitrification. *Water Environment Research* 80 (11):2145-2156.

177 Kies, F., S. Gillot, and A. Heduit. 2005. Paramètres influençant le transfert d'oxygène en
178 biofiltres. *Récents progrès en génie des procédés* 92.
179 Lang, L., M. Pocquet, B. Ni, Z. Yuan, and M. Sperandio. 2016. Comparison of different 2-
180 pathway models for describing the combined effect of DO and nitrite on the nitrous
181 oxide production by ammonia-oxidizing bacteria. *Water Science & Technology*.
182 Pocquet, M., Z. Wu, I. Queinnec, and M. Sperandio. 2016. A two pathway model for N2O
183 emissions by ammonium oxidizing bacteria supported by the NO/N2O variation.
184 *Water Research* 88:948-959.
185 Sabba, F., C. Picioreanu, J. P. Boltz, and R. Nerenberg. 2017. Predicting N2O emissions from
186 nitrifying and denitrifying biofilms: a modeling study. *Water Sci Technol* 75
187 (3):530-538.
188 Sander, R. 2015. Compilation of Henry's law constants (version 4.0) for water as solvent.
189 *Atmospheric Chemistry and Physics* 15 (8):4399-4981.
190 Vigne, E., J. M. Choubert, J. P. Canler, A. Heduit, K. Sorensen, and P. Lessard. 2010. A
191 biofiltration model for tertiary nitrification of municipal wastewaters. *Water*
192 *Research* 44 (15):4399-4410.